JOURNAL OF APPLIED ELECTROCHEMISTRY 19 (1989) 823–828

Mass transfer to and copper deposition on a round bar in a new type of electrolytic cell: the helix cell

L. J. J. JANSSEN, J. G. WIJERS

Faculty of Chemical Technology, Eindhoven University of Technology, PO Box 513, 5600 MB Eindhoven, The Netherlands

Received 22 September 1988; revised 23 January 1989

High-rate electrodeposition of copper from $CuSO_4$–H_2SO_4 baths can be achieved by using crossflow of solution. To obtain copper layers of uniform thickness and quality, a new type of electrolytic cell, the helix cell, has been proposed. An experimental dimensionless relation has been given to describe the mass transfer to a round bar, in crossflow, in a helix cell. Moreover, the current efficiency of copper deposition has been obtained as a function of current density, flow rate of solution, temperature and weight per cent $CuSO_4$ in the $CuSO_4$–H_2SO_4 solution.

Nomenclature

A_e	working-electrode surface area (m^2)
c	concentration of Cu^{2+} ($mol\,m^{-3}$)
c_e	c at electrode surface ($mol\,m^{-3}$)
c_b	c in bulk of solution ($mol\,m^{-3}$)
C	constant factor (–)
d_c	inner diameter of central cylinder of helix cell (mm)
d_h	volumetric hydraulic diameter of helix cell (mm)
d_s	width of helical slots in central cylinder of helix cell (mm)
d_w	diameter of working electrode (round bar) (mm)
D_i	diffusion coefficient of species i ($m^2\,s^{-1}$)
F	Faraday constant ($C\,mol^{-1}$)
I	current (A)
k_i	mass-transfer coefficient for a species i ($m\,s^{-1}$)
i	current density ($kA\,m^{-2}$, $A\,m^{-2}$)
L_c	length of working-electrode compartment of helix cell (m)
n	number of electrons involved in electrode reaction (–)
n_1, n_2, n_3	constants (–)
R	gas constant: $R = 8.31\,J\,K^{-1}\,mol^{-1}$
Re	Reynolds number: $Re = v_c d_h/v$ (–)
Sc	Schmidt number: $Sc = v/D$ (–)
Sh	Sherwood number: $Sh = kd_h/D$
t	time (s)
T	temperature (K)
U_s	volumetric rate of solution through the helix cell ($m^3\,s^{-1}$)
v_c	flow rate of solution through working-electrode compartment of the helix cell ($vc = U/(d_c - dw)Lc$) ($m\,s-1$)
ϱ	*density of solution* ($kg\,m^{-3}$)
μ	*dynamicviscosityofsolution*($kg\,m-1\,s-1$)
ν	*kinematic viscosity of solution* ($m2\,s-1$)
η_i	*current efficiency for formation of a species i* (–)

1. Introduction

Electrodeposition of copper on bars is often carried out in cupric sulphate–sulphuric acid baths at approximately $3\,kA\,m^{-2}$. Higher rates for the electrodeposition of copper on a round bar can be achieved by using crossflow of solution [1]. In industrial practice, however, the cell in [1] is not useful for electrodeposition of copper on bars due to non-uniform distribution of current across is cylindrical surface. To overcome this shortcoming, a new electrolytic cell – the helix cell – has been designed by the first-named author of this paper.

In this study, the characteristic of the mass transfer to a round bar in a helix cell has been investigated. Moreover, the current efficiency for copper deposition from a $CuSO_4$–H_2SO_4 bath has been determined for a wide range of parameters.

2. Experimental details

The cross-section of a helix cell is shown schematically in Fig. 1. The separate parts of the cell are presented in Fig. 2. The cell consists of two concentric cylinders, viz. the central cylinder with two helical slots and the outer cylinder. The cylindrically working electrode is placed in the middle of the central cylinder. The inner length of both cylinders, L_c, is 60 mm. The inner diameter of the central cylinder, d_c, varies from 11–19 mm and the outer diameter for all the central

0021-891X/89 $03.00 + .12

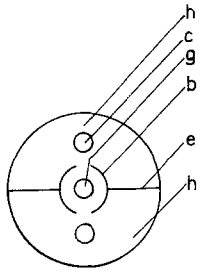

Fig. 1. Cross-section of the helix cell; b, central tube; c, counter-electrode; e, separation wall; g, working electrode; h, outer compartment.

cylinders is 24 mm. The helical slots, opposite each other, have a width, d_s, of between 2.4–6.0 mm and a pitch of 50 mm. The space between the central and the outer cylinder is divided into two equal counter-electrode compartments by a spiralled Perspex wall. The solution enters one counter-electrode compartment, flows subsequently through one helical slot, the working-electrode compartment and through the other helical slot into the other counter-electrode compartment. The working electrode is a platinum tube 9 mm in outer diameter, 60 mm in length and 17×10^{-4} m^2 in electrode surface area. The platinum tube was polished with diamond paste before its positioning in the cell. The wall thickness of the platinum tube is 0.25 mm. There is a current connection at each end of the platinum tube. It was shown that the ohmic potential drop across the platinum tube is negligible even at the highest current (25 A) applied. Two spiralled copper rods, 5 mm in diameter, served as the counter-electrode; one rod was placed in each counter-electrode compartment. The temperature of the solution was measured in the overflow vessel and maintained at a constant value to within 1° C. A common

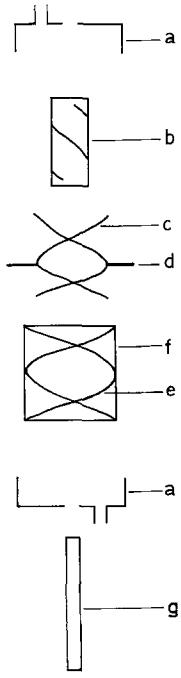

Fig. 2. Separate parts of the helix cell; a, cap with liquid inlet; b, Perspex cylinder with slots; c, Cu bars; d, current connection bars; e, spiral separation wall; f, outer wall of cell; g, working electrode.

circuit of solution for forced convection conditions was used. A solution of about 0.01 m^3 was pumped through a circuit consisting of electrolytic cell, overflow vessel, heat exchanger, pump and flowmeters.

The flow rate of solution in the working-electrode compartment at the cross-section, v_c, is equal to the volumetric rate of solution, U_s, through the cell, divided by the difference between the cross-section of the working-electrode compartment and that of the working electrode, both in the direction of the axis of the working electrode.

To visualize the pattern of the solution flow, the cell and the solution circuit were filled with water and a small quantity of blue ink was injected. It was observed that the whole length of both slots was practically uniformly used for solution flow.

It is noted that the helix cell can only be used to obtain equal thicknesses of copper deposition around a bar when the bar is transported through the helix cell.

To determine the mass-transfer characteristics, 1 M H_2SO_4 or sulphuric 4 M H_2SO_4, each containing 2.5 mM $CuSO_4$, were used. The solution was made oxygen-free by nitrogen gas bubbling. The current-efficiency measurements were carried out with $CuSO_4$/H_2SO_4 solutions with various contents of both species. The chosen contents are based on solubility data for the tertiary system $CuSO_4$–H_2SO_4–H_2O [2].

Mass-transfer and current-efficiency measurements were carried out in a similar fashion to that described previously [1]. The voltammograms were measured potentiodynamically at a scan rate of 50 mV s^{-1}. The scan started at a potential of 500 mV against saturated calomel electrode which was used as the reference electrode; before taking up a voltammogram, the working platinum electrode was made copper-free by anodic polarization at 500 mV against saturated calomel electrode.

3. Results and discussion

3.1. *Mass transfer*

Figure 3 shows two typical voltammograms for the cylindrical platinum electrode in oxygen-free 1 M H_2SO_4 solutions; one without $CuSO_4$ and the other containing 2.5 mM $CuSO_4$. The curve for the $CuSO_4$–H_2SO_4 solutions shows a pre-wave at potentials between 0.15 and 0.0 V; its limiting current is almost independent of the solution-flow rate. Moreover, this wave cannot be caused by reduction of dissolved oxygen. In mass-transfer studies, the potential–current curves for copper deposition are not given [3] or given only in the potential range where the limiting diffusion current occurs [4] or for relatively high $CuSO_4$ concentrations where the effect of the pre-wave is negligible. The pre-wave is caused by underpotential deposition of copper on the bare platinum surface [5]. Since the limiting current region of the current–potential curve Cu^{2+} reduction to Cu show no well-shaped plateau, determination of the limiting current poses

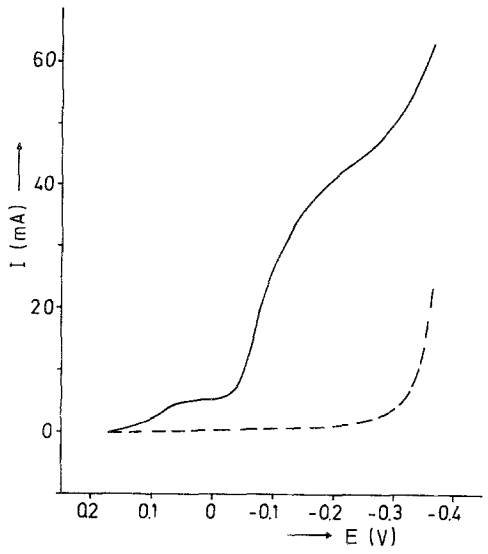

Fig. 3. Voltammograms for the cylindrical platinum electrode in oxygen-free 1 M H_2SO_4 solutions with (solid line) and without (dotted line) addition of 2.5 mM $CuSO_4$. Inner diameter of central cylinder: 15 mm. Width of slot in central cylinder: 2.4 mm. Temperature: 298 K, volumetric flow rate of solution: 0.13×10^{-3} m^3 s^{-1}.

some problems. The current at the inflection point of the potential–current curves may be accepted as the limiting current, in accord with general practice. The occurrence of the pre-wave has not been taken into account in the determination of the limiting diffusion current of Cu^{2+} ions because of the explanation of its occurrence. Moreover, unrealistic results are obtained when the pre-wave is taken into account.

The thickness of the Cu layer present on the smooth Pt tube after the measuring of the voltammogram was very low, namely lower than about 4×10^{-3} μm. Consequently, the nature of the copper deposit had no effect upon the mass-transfer data.

The reported values for the diffusion coefficient of Cu^{2+} are scattered over a surprisingly wide range. In particular, rotating disc determinations show the most scatter [4].

The recently published data on the diffusion coefficient of $CuSO_4$ in aqueous solutions at $T = 298$ K are discussed and new reliable results are given [4]. From [4] it follows that $D_{Cu^{2+}} = \{7.35 - 5.3 c_b^{0.5}\} \times 10^{-10}$ m^2 s^{-1} in a $CuSO_4$ solution containing 0.1 M H_2SO_4 at 298 K. From this relation for $D_{Cu^{2+}}$ and since the effect of the viscosity of sulphuric acid solutions is in agreement with the Stokes–Einstein equation [3], it has been calculated that $D_{Cu^{2+}}$ for a 2.5 mM $CuSO_4$ + 1.0 M H_2SO_4 solution at 298 K is 6.1×10^{-10} m^2 s^{-1} and for a 2.5 mM $CuSO_4$ + 4.0 M H_2SO_4 solution at 298 K is 3.8×10^{-10} m^2 s^{-1}.

Since no reliable results are available on the diffusion coefficient of Cu^{2+} ions in sulphuric acid solutions over a wide range of temperature, it is assumed that the temperature dependence of $D_{Cu^{2+}}$ in sulphuric acid solutions is equal to that found for 0.0625 M $CuSO_4$ [5]. From results of [5] it was shown that, in the temperature range from 300–330 K, the activation energy for diffusion of Cu^{2+} ions is 22.21 kJ mol^{-1}.

Table 1. Diffusion coefficient for Cu^{2+} in 1.0 M and 4.0 M H_2SO_4 solution, containing *2.5 mM $CuSO_4$ at various temperatures*

	$D_{Cu}(II) \times 10^{10}$ m^2 s^{-1}	
Temperature (T/K)	*1 M H_2SO_4*	*4 M H_2SO_4*
298	6.1	3.8
308	8.2	5.1
323	12.2	7.6
343	19.8	12.3

The calculated diffusion coefficient of $D_{Cu(2+)}$ for two solutions at various temperatures is given in Table 1.

To describe mass-transfer characteristics in electrolytic cells, the Sherwood number, Sh, the Reynolds number, Re, and the Schmidt number, Sc, are used frequently. The Sherwood number, Sh, is kd_h/D where k is the mass-transfer coefficient on a circumference-average basis for the working electrode.

The determination of the mass-transfer coefficient is described in [1]. The kinematic viscosity of 1 M H_2SO_4 and 4 M H_2SO_4 at various temperatures is obtained from [7, 8] and tabulated in Table 1.

The volumetric hydraulic diameter is defined by $d_h = 4 \times$ volume of free space for the flow divided by the area of the wetted surface. It can be shown that for the helix cell $d_h = d_c - d_w$.

The Reynolds number is defined by $\mathrm{Re} = v_c d_h/\nu$. The solution-flow rate v_c in the working-electrode compartment is given by $v_c = U_s/(d_c - d_w)L_c$ and the Reynolds number by $\mathrm{Re} = U_s/\nu L_c$.

Figure 4 shows Sh as a function of Re on a double logarithmic plot for a 2.5 mM $CuSO_4$ + 1 M H_2SO_4 solution at various temperatures. From this figure it follows that the log Sh/log Re curves are parallel to one another, the slope n_1 of a log Sh/log Re curve increases with increasing Re and n_1 only depends on Re.

Figure 5 shows Sh as a function of Sc on a double logarithmic scale for a 1 M and 4 M H_2SO_4 solution, containing 2.5 mM $CuSO_4$. The change in the Schmidt

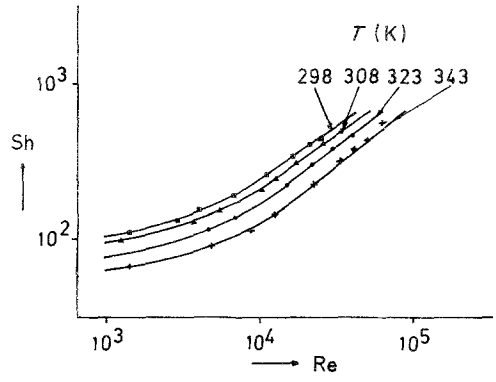

Fig. 4. Sherwood number as a function of Reynolds number for a working cylindrical platinum electrode in 1.0 M H_2SO_4 containing 2.5 mM $CuSO_4$ and at various temperatures. The diameter of the working electrode is 9.0 mm, the inner diameter of the central cylinder is 15 mm and the width of the helical slot in the central cylinder is 4.3 mm.

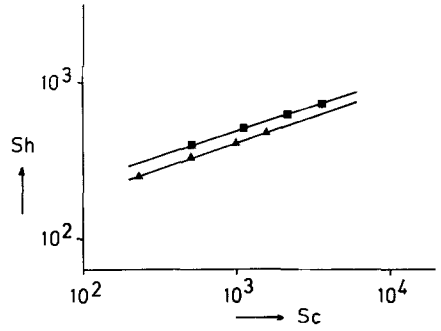

Fig. 5. Sherwood number as a function of Schmidt number for a working cylindrical platinum electrode in 1.0 and 4.0 M H_2SO_4, each containing 2.5 mM $CuSO_4$. Diameter of working electrode 9.0 mm; inner diameter of central cylinder 15 mm; width of helical slot in central cylinder 4.3 mm. ■ 4 M H_2SO_4; ▲ 1 M H_2SO_4.

number was obtained by changing the solution temperature. The two straight lines are parallel, their slope, n_2, being 0.33. This value of slope is quite common for forced convection mass transfer [9] and for wire electrodes in electroplating cells of various designs [10].

It is likely that the observed difference in the positions of the lines is caused by inaccuracies in diffusion coefficient, kinematic viscosity, solution-flow rate and/or limiting current of Cu deposition.

The effect of the diameter of the helical slot, d_s, and the inner diameter of the central tube, d_c, on the Sherwood number at a constant volumetric flow rate of solution, viz. respectively 100 to 150 $cm^3\ s^{-1}$, and at various temperatures, is shown in Figs 6 and 7. From these figures it follows that the Sherwood number does not depend on d_s at $d_s > 3.5$ mm and on d_c at $d_c > 14$ mm. Plotting Sh versus Re on a double logarithmic scale, it has been found that the slope, n_1, is practically independent of d_s as well as d_c.

Summarizing the experimental data on mass transfer to a working cylindrical electrode in a helix cell, it follows that

$$Sh = C\,Re^{n_1}Sc^{1/3} \qquad (1)$$

where the constants C and n_1 depend only on Re for a helix cell with $d_s > 3.5$ mm and $d_c > 14$ mm. A similar relation has been found for the average heat-transfer coefficient for a heated cylinder in cross-flow with a constant solution-flow rate outside the boundary.

From Fig. 4 it can be calculated that

$$Sh = 0.017\,Re^{0.76}Sc^{1/3} \qquad (2)$$

and

$$Sh = 0.011\,Re^{0.81}Sc^{1/3} \qquad (3)$$

at, respectively, $Re = 2 \times 10^4$ and 5×10^4.

Since the slope n_1 increases with increasing Re, a more practical relation is desirable. The experimental results of Fig. 4 are presented in Fig. 8 by plotting $Sh-Sh_0$ against Re on a double logarithmic scale where Sh_0 is the extrapolated Sh at $Re = 0$. From Fig. 8 it follows that the curves are linear and parallel. From this figure and Sh_0 derived from Fig. 4, it follows that, for the Re range between 3×10^3 and 7×10^4

$$Sh = (10.0 + 5.72 \times 10^{-4}\,Re^{1.08})Sc^{0.33}. \qquad (4)$$

The relation for Sh is useful for helix cells with $d_s > 3.5$ mm and $d_c > 14$ mm and $d_w = 9$ mm.

The effect of the diameter of the cylindrical working electrode has not been investigated since electrodes with various diameters were not available.

Grassmann *et al.* have studied mass transfer to a cylinder electrode in cross flow [10]. They found that Sh is proportional to Re^{n_3} for cylindrical working electrodes of 5 and 10 mm diameter in cross flow. The diameter of the electrode was used as the characteristic length to calculate the Reynolds number. They used a tube of 50 mm as the electrolytic cell. The working electrode was mounted perpendicularly to the axis of this 50 mm tube. They found that the coefficient n_3 increased markedly with increasing Re; $n_3 = 0.44$ for $160 < Re < 1000$ and 0.56 for $1000 < Re < 12600$. For the helix cell a similar relationship between Re and Sh has been obtained (Fig. 4). Tvarusko [11] has investigated mass transfer to a wire (0.25 mm in diameter) in cross flow. Tvarusko's electrolytic cell was similar to that used by Grassmann *et al.* He found that

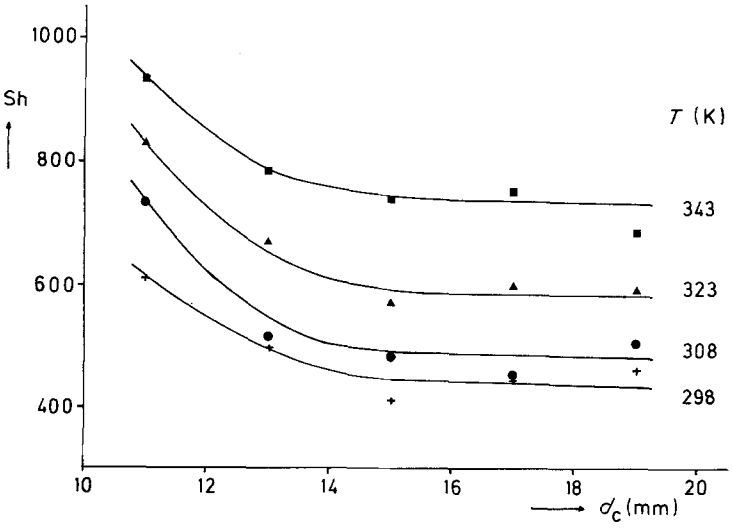

Fig. 6. Sherwood number as a function of the inner diameter of the central Perspex cylinder of the helix cell for a working cylindrical platinum electrode (diameter 9.0 mm) in a 2.5 mM $CuSO_4$ + 1 M H_2SO_4 solution at various temperatures. Width of helical slot 4.3 mm; volumetric flow rate $0.15 \times 10^{-3}\ m^3\ s^{-1}$.

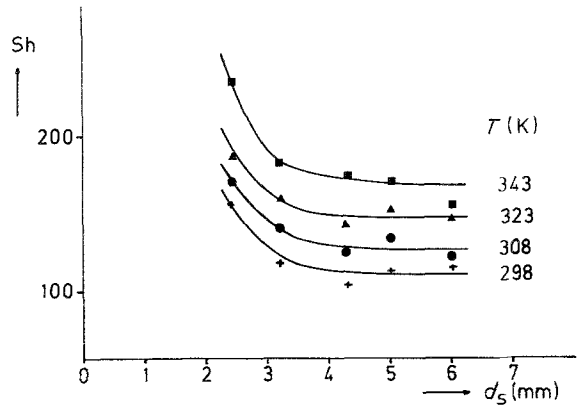

Fig. 7. Sherwood number as a function of the width of the helical slot in the central Perspex cylinder of the helix cell for a working cylindrical platinum electrode (diameter 9.0 mm) in a 2.5 mM $CuSO_4$ + 1 M H_2SO_4 solution at various temperatures. Inner diameter of central Perspex cylinder 15 mm; volumetric flow rate 0.10×10^{-3} m^3 s^{-1}.

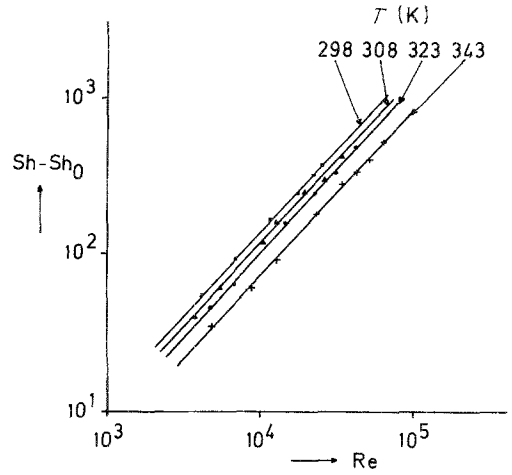

Fig. 8. The difference Sh–Sh$_0$ plotted against Re on a double logarithmic scale for a working cylindrical platinum electrode. Conditions as for Fig. 4.

Sh is proportional to $Re^{0.49}Sc^{0.33}$ for Reynolds numbers between 100–200. It should be noted that the design of the helix cell is completely different from that used by Grassmann *et al.*

The data on mass transfer to the cylinder working electrode in a helix cell are practically unaffected by entrance length effects, when the difference in pressure over each of the two counter-electrode compartments is much lower than that between both the counter-electrode compartments. The dimensions of some parts of the helix cell, for instance the width of the helical slots and the diameter of the central tube, the working electrode and of the outer cylinder, strongly affect the differences in pressure inside the helix cell.

From the solution flow pattern in the helix cell used, it can be concluded that the entrance effects do not affect the mass-transfer data. These data do not depend on the length of the electrolytic cell.

3.2. *Current efficiency for copper deposition*

The current efficiency, η_{Cu}, for copper deposition during cathodic polarization of a round bar were determined as described in [1]. Experiments were carried out with solutions containing various concentrations of $CuSO_4$ and H_2SO_4 and at current densities from 5–20 kA m^{-2}, solution flow rates, v_c, from 0.07 to 0.50 m s^{-1} and at temperatures from 303–343 K. The helix cell used for current efficiency measurements had a central tube with an inner diameter of 15 mm and two spiralled slots with a 4.3 mm width in the central tube.

To minimize the resistivity of the $CuSO_4$–H_2SO_4 solution, the concentration of H_2SO_4 was maximal at a fixed $CuSO_4$ concentration for a temperature of 288 K. The composition numbers of the $CuSO_4$–H_2SO_4 solution used were 15.0/2.0, 12.5/5.0, 10.7/10.0 and 9.3/15.0, where the first number of the combination indicates the weight per cent of $CuSO_4$ and the second the weight per cent of H_2SO_4.

Figure 9 shows η_{Cu} as a function of current density for solutions of various compositions and at a solution flow rate v_c = 0.37 m s^{-1} and T = 323 K. The visually observed formation of dendrites occurs in the region below the dotted line of Fig. 9. This line is only a rough indication for the boundary of formation of copper dendrites. This region is also indicated in Figs 10 and 11. Figure 10 shows the effect of the flow rate of solution, v_c, for the 12.5/5 solution at various current densities and 323 K.

The effect of temperature is shown in Fig. 11 for solutions of various compositions and at 10 kA m^{-2}

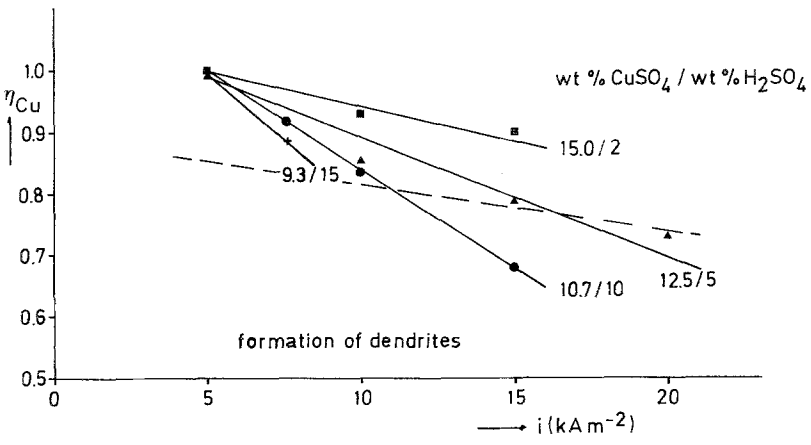

Fig. 9. Copper current efficiency as a function of current density during copper deposition on a round bar at a solution flow rate of 0.37 m s^{-1} and a temperature of 323 K and in various compositions of the $CuSO_4$–H_2SO_4 bath.

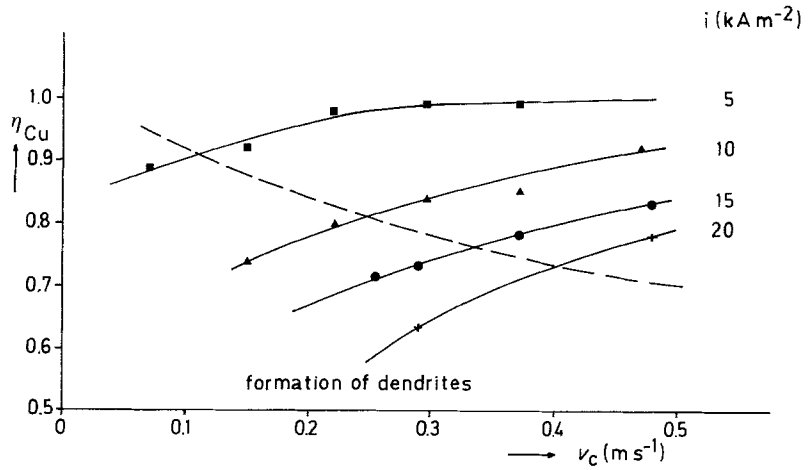

Fig. 10. Copper current efficiency as a function of flow rate of solution during copper deposition on a round bar in a solution containing 12.5 weight per cent $CuSO_4$ and 5.0 weight per cent H_2SO_4 at various current densities and at 323 K.

and $v_c = 0.37\,m\,s^{-1}$. From Figs 9–11 it follows that the current efficiency for copper deposition increases with increasing $CuSO_4$ concentration, temperature and flow rate of solution and with decreasing current density.

From the experimental results, a correlation for the current efficiency for copper deposition on a round bar 9 mm in outer diameter in a helix cell with 15 mm in inner diameter and 4.3 mm in width of slot has been deduced. This correlation is given by

$$\frac{\eta_{Cu}}{1-\eta_{Cu}} = 10.6[i^{-1.6}]10^{0.57v_c} + 9.8X_1 - 2.0 \times 10^3 \times \left(\frac{1}{T} - \frac{1}{323}\right) \quad (5)$$

where i is in $kA\,m^{-2}$; v_c in $m\,s^{-1}$; T in K; X_1 weight per cent $CuSO_4$ in $CuSO_4/H_2SO_4$ solution.

Similar results have been obtained with another type of cell [1] where the solution flow was also directed normal to the axis of a round bar. The main difference between the types of cell is the shape of the slots in the central cylinder, viz., helical slots in the helix cell and rectangular slots in the other.

From the results on mass transfer to a round bar in a helix cell with central cylinders of various inner diameters and with central cylinders having slots differing in width, it follows that the current efficiency for copper deposition increases with decreasing gap width between the round bar and the central cylinder and with decreasing width of slots in the central cylinder. From the current efficiency and mass-transfer experiments it follows that very high rates of copper deposition, e.g. higher than $10\,kA\,m^{-2}$, for the $CuSO_4$–H_2SO_4 baths used in practice can be achieved with helix cells where the solution flow is directed to the axis of a round bar. Because of the configuration of the helix cell, a round bar can be covered with a copper layer of uniform thickness when the bar is transported through the helix cell.

References

[1] L. J. J. Janssen, *J. Appl. Electrochem.* **18** (1988) 339.
[2] G. Agde and H. Barkholt, *Z. Angew. Chem.* **40** (1927) 374.
[3] A. J. Arvia, J. C. Barim and J. S. W. Carroza, *Electrochim. Acta* **11** (1966) 881.
[4] T. I. Quickenden and X. Jiang, *Electrochim. Acta* **29** (1984) 693.
[5] G. W. Tindall and S. Bruckenstein, *Anal. Chem.* **40** (1968) 1051.
[6] R. N. O'Brien and C. Rosenfield, *J. Phys. Chem.* **67** (1963) 643.
[7] J. G. Knudsen and D. L. Katz, 'Fluid Dynamics and Heat Transfer', McGraw-Hill Book Co., New York (1958) pp. 81–82.
[8] E. W. Washburn, 'International Critical Tables', Vol. V, 12. McGraw-Hill Book Company, New York and London, 1929.
[9] Landolt Bornstein, 'Zahlenwerte und Funktionen aus Physik, Chemie, Astronomie, Geophysik and Technik', Springer Verlag, Berlin, II. Band, 5. Teil, Bandteil a (1969) 631.
[10] D. J. Pickett, 'Electrochemical Reactor Design', 2nd edn, Elsevier Scientific Publishing Company, Amsterdam (1977).
[11] P. Grassmann, N. Ibl and J. Trüb, *Chem. Ing. Tech.* **33** (1961) 529.
[12] A. Tvarusko, *J. Electrochem. Soc.* **120** (1973) 87.

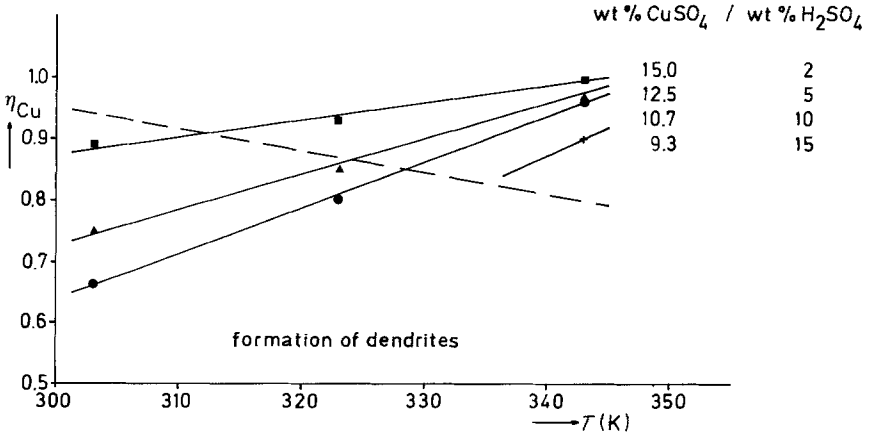

Fig. 11. Copper current efficiency as a function of temperature during copper deposition on a round bar in a solution containing various concentrations of H_2SO_4 and $CuSO_4$, at a current density of $10\,kA\,m^{-2}$ and a solution flow rate of $0.37\,m\,s^{-1}$.